**Aalborg Universitet**

# Predicting glyphosate sorption across New Zealand pastoral soils using basic soil properties or Vis–NIR spectroscopy

Hermansen, Cecilie; Norgaard, Trine; Wollesen de Jonge, Lis; Moldrup, Per; Müller, Karin; Knadel, Maria

# Predicting glyphosate sorption across New Zealand pastoral soils using basic soil properties or Vis–NIR spectroscopy

Cecilie Hermansen[a],[*], Trine Norgaard[a], Lis Wollesen de Jonge[a], Per Moldrup[b], Karin Müller[c], Maria Knadel[a]

[a] *Dept. of Agroecology, Faculty of Sciences and Technology, Aarhus University, Blichers Allé 20, P.O. Box 50, DK-8830 Tjele, Denmark*
[b] *Dept. of Civil Engineering, Aalborg University, Thomas Manns Vej 23, DK-9200 Aalborg, Denmark*
[c] *The New Zealand Institute for Plant & Food Research Limited (PFR), Land Use Impacts, Hamilton, New Zealand*

A B S T R A C T

Glyphosate [N-(phosphonomethyl) glycine] is the active ingredient in Roundup, which is the most used herbicide around the world. It is a non-selective herbicide with carboxyl, amino, and phosphonate functional groups, and it has a strong affinity to the soil mineral fraction. Sorption plays a major role for the fate and transport of glyphosate in the environment. The sorption coefficient ($K_d$) of glyphosate, and hence its mobility, varies greatly among different soil types. Determining $K_d$ is laborious and requires the use of wet chemistry. In this study, we aimed to estimate $K_d$ using basic soil properties, and visible near-infrared spectroscopy (vis–NIRS). The latter method is fast, requires no chemicals, and several soil properties can be estimated from the same spectrum. The data set included 68 topsoil samples collected across the South Island of New Zealand, with clay and organic carbon (OC) contents ranging from 0.001 to 0.520 kg kg$^{-1}$ and 0.021 to 0.217 kg kg$^{-1}$, respectively. The $K_d$ was determined with batch equilibration sorption experiments and ranged from 13 to 3810 L kg$^{-1}$. The visible near-infrared spectra were obtained from 400 to 2500 nm. Multiple linear regression was used to correlate $K_d$ to oxalate extractable aluminium and phosphorous and pH, which resulted in an $R^2$ of 0.89 and an RMSE of 259.59 L kg$^{-1}$. Further, interval partial least squares regression with ten-fold cross-validation was used to predict $K_d$ by vis–NIRS, and an $R^2$ of 0.93 and an RMSECV of 207.58 L kg$^{-1}$ were obtained. Thus, these results show that both basic soil properties and vis–NIRS can predict the variation in $K_d$ across these samples with high accuracy and hence, that glyphosate sorption to a soil can be determined with vis–NIRS.

## 1. Introduction

Glyphosate is a non-selective, broad-spectrum herbicide, which is intensively used for weed control worldwide (Borggaard and Gimsing, 2008). In fact, it is the most widely used herbicide in the world, and also in New Zealand, where it is used in about 90 different herbicides (Ministry for Primary Industries, 2015). The last survey of pesticide use in New Zealand was conducted in 2004: 344.3 t of the active ingredient were used which equals about 8% of the total pesticide use in 2004 (Manktelow et al., 2004). Glyphosate was the only pesticide determined in concentrations up to 950 ng g$^{-1}$ in sediment samples from estuarine sites located in residential areas of Auckland, New Zealand's biggest city (Stewart et al., 2014). However, in spite of its intensive use in agriculture and residential areas, the herbicide has not yet been included in the 4-yearly national survey of pesticide residues in groundwater (Close and Skinner, 2012).

Glyphosate sorbs strongly to soil. Despite this, glyphosate and its metabolite aminomethylphosphonic acid (AMPA) have also been detected in ground and surface waters (Borggaard, 2011; Borggaard and Gimsing, 2008; Kjær et al., 2005; Norgaard et al., 2014). This may partly be explained by colloid-facilitated transport of glyphosate (de Jonge et al., 2004a; de Jonge et al., 2004b; Norgaard et al., 2013). The mobility of glyphosate in soil and hence the risk of leaching depend *inter alia* on sorption-desorption processes, biological and chemical degradation, and leaching through the soil matrix or macropores either in dissolved form or sorbed onto colloids (Al-Rajab et al., 2008; Arias-Estévez et al., 2008; Borggaard and Gimsing, 2008; de Jonge et al., 2000; Norgaard et al., 2014).

The sorption coefficient ($K_d$) is one of the most important soil properties for assessing the risk of pesticide leaching (Farenhorst et al.,

---

2008). Glyphosate is composed of three functional groups (amino, phosphonate and carboxylate), and it sorbs strongly to the soil mineral fraction with high affinity for iron and aluminum oxides (Borggaard, 2011; de Jonge et al., 2001; Gerritse et al., 1996; Sheals et al., 2002) and clay minerals (Borggaard and Gimsing, 2008; Glass, 1987; Sprankle et al., 1975). The literature on the effect of soil organic matter (OM) on the $K_d$ of glyphosate report contrasting results (Borggaard and Gimsing, 2008; Vereecken, 2005): It was reported that OM can increase $K_d$ (Dollinger et al., 2015; Piccolo et al., 1996), have no effect, or decrease $K_d$ (Gerritse et al., 1996; Paradelo et al., 2015). The content of phosphate can decrease glyphosate sorption, because phosphate and glyphosate compete for the same sorption sites (Borggaard, 2011; de Jonge and de Jonge, 1999; de Jonge et al., 2001; Gimsing and Borggaard, 2010), although it has also been suggested that glyphosate and phosphate sorption can be additive (Borggaard and Gimsing, 2008).

Besides soil composition, soil chemistry also affect the $K_d$ of glyphosate. It is well documented that an increase in pH is accompanied by a decreasing $K_d$ of glyphosate (de Jonge and de Jonge, 1999; Gimsing et al., 2004; Paradelo et al., 2015). Glyphosate becomes more negatively charged with increasing soil pH, which increases the electrostatic repulsion between the negatively charged glyphosate and the soil surface (Dollinger et al., 2015). Cation exchange capacity is another factor which increases $K_d$ (Dollinger et al., 2015), whereas increasing electrical conductivity (EC) decreases $K_d$, which might be caused by cations in solution that forms a complex with glyphosate, and thereby reduces sorption to the soil (Paradelo et al., 2015).

The $K_d$ of glyphosate can be measured by batch equilibrium sorption experiments, and several authors suggest to estimate $K_d$ from pedotransfer-functions with a set of easily measurable soil properties as input parameters (Dollinger et al., 2015; Gimsing et al., 2004; Paradelo et al., 2015). Pedotransfer-functions have proven useful for determining $K_d$, but the optimal set of soil properties for $K_d$ determination depends on the specific dataset used (Paradelo et al., 2016). Prioritization of the soil properties required for estimating $K_d$ remains a complex task. Visible near-infrared spectroscopy (vis–NIRS) has also been used to predict sorption coefficients of pesticides (Bengtsson et al., 2007; Forouzangohar et al., 2009; Paradelo et al., 2016). It is a rapid and cost efficient alternative to conventional soil analysis. Multiple basic and functional soil properties can be predicted from one visible near-infrared (vis–NIR) spectrum (Ben-Dor and Banin, 1995; Chang et al., 2001; Hermansen et al., 2016; Hermansen et al., 2017; Katuwal et al., 2018a; Katuwal et al., 2018b; Knadel et al., 2016; Stenberg et al., 2010). Detailed information about the organic and inorganic soil composition is embedded in the vis–NIR spectra. This information originates from overtone and combination bands from fundamental vibrations of different functional groups (CO, CH, OH, NH, and metal-OH) in the mid-infrared range (Clark, 1999; Hunt, 1977). These spectral signatures enable the wide applicability of vis–NIRS to predict soil properties (Ben-Dor and Banin, 1995; Stenberg et al., 2010).

Only one previous study has documented successful vis–NIRS prediction of $K_d$ of glyphosate across a Danish agricultural field ($K_d$ from 162 to 536 L kg$^{-1}$) (Paradelo et al., 2016). Iron and aluminium oxides as well as clay minerals have been found to be some of the main controllers of the $K_d$ of glyphosate (Borggaard and Gimsing, 2008; Dollinger et al., 2015). These are soil properties with direct spectral signatures within the vis–NIR spectral range (Ben-Dor, 2002). Thus, there is a potential that vis–NIRS can predict the $K_d$ of glyphosate across soils with larger variability. In this study, we used soil samples from New Zealand collected across the entire South Island, thus representing a wide range of soil orders, parent materials and mineralogy. Our specific objectives were to:

i. Determine the set of soil properties that best describe the variation in the $K_d$ of glyphosate.
ii. Examine if the $K_d$ of glyphosate can be predicted based on vis–NIRS spectra.
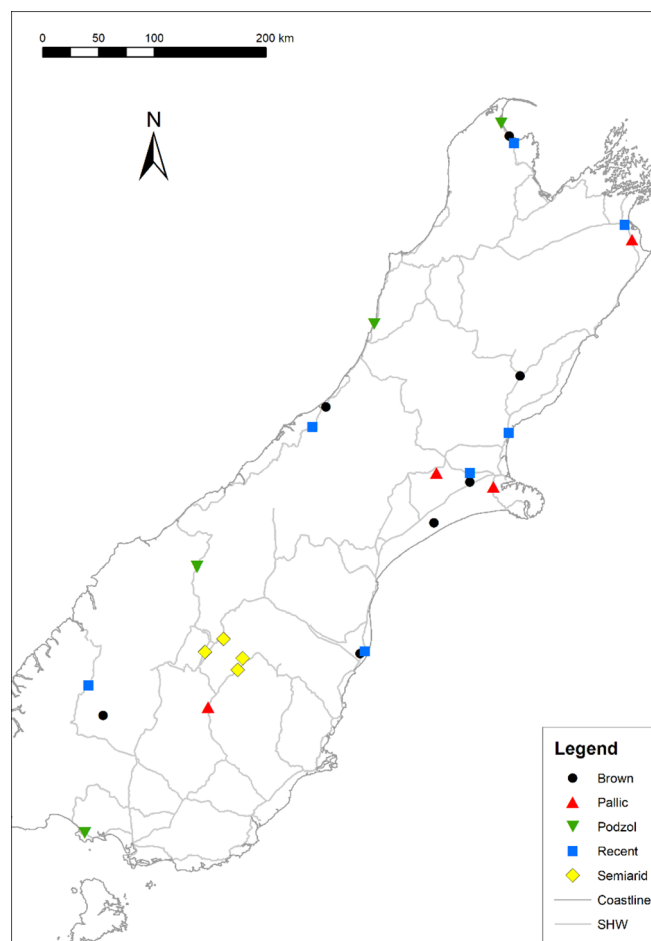


**Fig. 1.** Sampling sites at the South Island of New Zealand for the 68 soil samples included in this study. The twenty-six sampling sites represented five soil orders. SHW, state highway networks.

## 2. Materials and methods

### 2.1. Soil samples and soil properties

Soil samples were collected across New Zealand's South Island in summer 2012 (Hermansen et al., 2019). The 26 sampling sites were selected to represent the dominant soil orders under pasture in the island, being Brown, Pallic, Podzol and Recent soils (Hewitt, 2010). The soil order Semiarid was also included because it is the dominant soil order in one region (Fig. 1). In the classification of the World Reference Base for Soil Resources (IUSS Working Group WRB, 2006) these soil orders correspond to Cambisols, Luvisols, Podzols, Fluvisols and Arenosols, respectively. At each site, three bulk soil samples (0–5-cm depth) were taken along a transect of 30 m length. The soil samples were sieved to < 2 mm, air-dried, and analyzed for texture on a Malvern laser sizer (Mastersizer 2000, Malvern Instruments, Malvern, UK) and organic carbon (OC) content using a Leco Truspec instrument (Blakemore et al., 1987). The pH was measured in 1 M KCl following the methodology of Blakemore et al. (1987) and EC was measured in a soil/water extract of 1:9 by volume. Oxalate extractable iron ($Fe_{ox}$), aluminium ($Al_{ox}$) and phosphorous ($P_{ox}$) were measured following the method of Schoumans (2000), and Olsen P was measured following the method of Olsen (1954).

### 2.2. Determination of glyphosate sorption coefficient

For the determination of the $K_d$ of glyphosate, $^{14}$C labelled

glyphosate ([glycine 2-14C] glyphosate, N-(phosphonomethyl)glycine) was purchased from Perkin Elmer (Boston, USA). The $^{14}$C labelled glyphosate was dissolved in 0.01 M $CaCl_2$ to prepare stock solutions with an initial glyphosate concentration of 0.23 mg L$^{-1}$. To prevent microbial degradation, sodium azide (1.00 g L$^{-1}$) was added to the glyphosate solution (Soares et al., 2013).

The $K_d$ of glyphosate was measured with batch sorption experiments in triplicate. Soil aliquots of 0.5 g were transferred to glass centrifuge tubes with Teflon caps and equilibrated with 0.5 mL of 0.01 M $CaCl_2$ for 24 h. Nine milliliters of glyphosate stock solution (0.23 mg L$^{-1}$) were added, after which the samples were rotated end-over-end at 30 rpm at 20 °C for 24 h. Then, the samples were centrifuged at 5000 rpm for one hour. From each sample, three mL of the supernatant were mixed with 17 mL scintillation cocktail (Packard Ultima Gold). A liquid scintillation analyzer (Packard Tri-carb 2250CA, Packard Instrument Co., IL) was used to measure the activity of the solution (DPM) which was then transformed to concentration (g L$^{-1}$). The specific amount of glyphosate sorbed (Cs; g kg$^{-1}$) was calculated from the soil dry weight (ms) and the difference between the solution concentration (g L$^{-1}$) at apparent equilibrium (Ce) (i.e., after the 24-h incubation period) and the solution concentration (g L$^{-1}$) in equivalent samples from assays run without soil (Ci):

$$C_s = V(C_i - C_e)/m_s \qquad (1)$$

where V is the volume in liters. The sorption coefficient of glyphosate, $K_d$ (L kg$^{-1}$) was calculated from:

$$K_d = \frac{C_s}{C_e} \qquad (2)$$

### 2.3. Multiple linear regression analysis

A forward multiple linear regression (MLR) analysis was performed to find a subset among the measured basic soil properties (clay, silt, sand, OC, pH, EC, $Al_{ox}$, $Fe_{ox}$, $P_{ox}$, and Olsen P) that would control the variation in the $K_d$ of glyphosate across the 68 samples. In the MLR, it was a prerequisite that the effect of a given soil property was significant ($p < 0.05$) to be included. Further, the variance inflation factor (VIF) was used to indicate multicollinearity among the soil properties.

### 2.4. Vis–NIRS measurements

For this study, we used a NIRS$^{TM}$ DS2500 spectrometer (FOSS, Hillerød, Denmark). It measures diffuse reflectance in a sampling interval of 0.5 nm from 400 to 2500 nm (Hermansen et al., 2016). The instrument require approximately 30–50 g of air-dried and 2-mm sieved soil sample, which was transferred to a quartz sample cup with a cup diameter of 7 cm and a glass diameter of 6 cm. The cup was rotated inside the spectrometer, resulting in spectral measurements at seven positions. The seven scans were further averaged into one representative soil spectrum. The diffuse reflectance (R) was then converted into absorbance (A) (A = [log(1/R)]).

### 2.5. Multivariate data analysis

The Matlab program PLS Toolbox version 8.6.2 (Eigenvector Research Inc.) was used for multivariate data analysis. Partial least squares regression (PLSR) (SIMPLS algorithm; (de Jong, 1993) with ten-fold cross-validation was used to correlate the vis–NIR spectra to each of the soil properties to be predicted and thereby establish vis–NIRS prediction models. Different spectral preprocessing methods were applied to correct for nonlinear trends and additive and/or multiplicative effects in the spectrum, including Savitzky-Golay 1st and 2nd derivative (Savitzky and Golay, 1964), detrending, and standard normal variate (SNV) (Barnes et al., 1989). The regression coefficient from each model was used to indicate spectral bands important for predicting each soil property.

To further optimize the vis–NIRS model for pH, $P_{ox}$, $Fe_{ox}$, $Al_{ox}$, and the $K_d$ of glyphosate, the variable selection method "interval partial least square regression" (iPLSR) (Hermansen et al., 2017; Knadel et al., 2018; Nørgaard et al., 2000; Zou et al., 2010) was applied on pretreated spectra to test whether these parameters could be predicted with higher accuracy using only a subset of spectral intervals compared to using the entire spectrum. Previous studies have shown that using spectral intervals found by forward iPLSR can decrease prediction errors and at the same time sort out irrelevant spectral information for a specific soil property, thereby decreasing model complexity (Hermansen et al., 2017; Knadel et al., 2018).

The root mean square error (RMSE) of calibration (RMSEC) and cross-validation (RMSECV), the coefficient of determination ($R^2$), as well as the ratio of performance to interquartile range (RPIQ) were used as statistical measures to evaluate model accuracy. The RPIQ relates the RMSECV to the difference between the third (Q3) and first (Q1) quartile of the dataset (RPIQ = (Q3 − Q1/RMSECV) (Bellon-Maurel et al., 2010).

## 3. Results and discussion

### 3.1. Soil properties and glyphosate sorption

This dataset represented five soil orders (Brown, Pallic, Podzol, Recent, and Semiarid) (Fig. 1) within the New Zealand soil classification scheme and thereby the soils covered a wide range in mineralogy and USDA texture classes (Table 1; Fig. 2). Eight soil types were represented (sand, loamy sand, sandy loam, loam, silty loam, silt, silty clay loam, and silty clay), with clay contents between 0.001 and 0.520 kg kg$^{-1}$ and OC contents between 0.021 and 0.217 kg kg$^{-1}$ (Table 1). The $K_d$ of glyphosate spanned a wide range from 13.4 to 3810.4 L kg$^{-1}$ (Table 1). In comparison, the study of Dollinger et al. (2015) represented soils from 23 studies conducted in Asia, Europe, and South and North America with a gradient in the $K_d$ of glyphosate of 0.06 to 403.5 L kg$^{-1}$, and the study of Paradelo et al. (2015) included two Danish field sites with $K_d$ of glyphosate between 161 and 667 L kg$^{-1}$).

The soil property with the highest correlation to the $K_d$ of glyphosate was $Fe_{ox}$, ranging from 8.9 to 260.0 mmol kg$^{-1}$ (r = 0.91,

**Table 1**
Descriptive statistics of selected soil properties for New Zealand soil samples.

| | Clay Kg kg$^{-1}$ | Silt Kg kg$^{-1}$ | OC[a] Kg kg$^{-1}$ | pH | EC[b] mS cm$^{-1}$ | $Al_{ox}$[c] mmol kg$^{-1}$ | $Fe_{ox}$[c] mmol kg$^{-1}$ | $P_{ox}$[c] mmol kg$^{-1}$ | Olsen P[d] mmol kg$^{-1}$ | $K_d$[e] L kg$^{-1}$ |
|---|---|---|---|---|---|---|---|---|---|---|
| Min | 0.001 | 0.064 | 0.021 | 4.5 | 0.6 | 7.6 | 8.9 | 6.2 | 0.4 | 13.4 |
| Max | 0.520 | 0.896 | 0.217 | 6.3 | 10.0 | 340.0 | 260.0 | 68.0 | 7.1 | 3810.4 |
| Mean | 0.088 | 0.632 | 0.056 | 5.3 | 3.4 | 78.6 | 63.3 | 22.2 | 1.7 | 690.1 |

[a] OC, Organic carbon.
[b] EC, Electrical conductivity.
[c] $Al_{ox}$, $Fe_{ox}$ and $P_{ox}$, Oxalate-extractable aluminum, iron and phosphorous.
[d] Olsen P, plant available phosphorous.
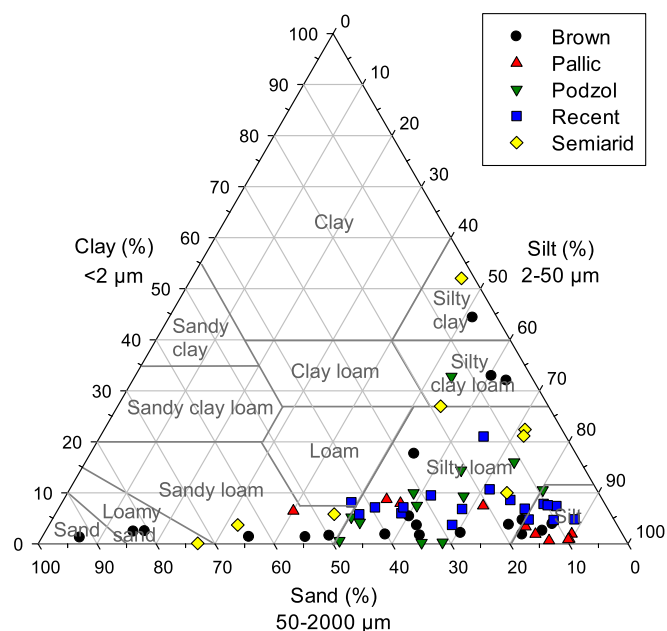[e] $K_d$, glyphosate sorption coefficient.

**Fig. 2.** Distribution of the soil samples from New Zealand (n = 68) within the USDA soil textural triangle.

p < 0.001) closely followed by $Al_{ox}$ ranging from 7.6 to 340.0 mmol kg$^{-1}$ (r = 0.89, p < 0.001) (Table 2; Fig. 3c and d). This finding corroborates with the literature: The variable-charge surfaces of aluminum and iron oxides are known to be amongst the main sorbents for glyphosate in soil (Borggaard and Gimsing, 2008; Gimsing and Borggaard, 2010). The content of $P_{ox}$ (6.2–68.0 mmol kg$^{-1}$) as well as pH (4.5–6.3) also contributed to explaining the variation in the $K_d$ of glyphosate (r = 0.37, p < 0.01 and r = -0.26, p < 0.05, respectively) of these acidic soils (Table 2; Fig. 3a and b). Surprisingly, clay content did not correlate to the $K_d$ of glyphosate (Table 2), although it has been found to be an important sorbent for glyphosate in other studies (Dollinger et al., 2015; Paradelo et al., 2015). This might be explained by the potentially wide variability in mineralogy amongst the soils of our dataset. Differences in glyphosate sorption capacity of clay minerals have been observed: Glass (1987) found montmorillonite to exhibit the highest capacity for glyphosate sorption followed by illite and then kaolinite, and Gimsing and Borggaard (2010) also found montmorillonite to sorb more glyphosate compared to illite.

### 3.2. Multiple linear regression analysis

The forward MLR revealed that the variation in the $K_d$ of glyphosate could be explained using $Fe_{ox}$, $Al_{ox}$, $P_{ox}$, and pH in combination. However, the intercorrelation between $Al_{ox}$ and $Fe_{ox}$ was high (VIF of 6.4 and 6.4, respectively) (Table 2), and therefore $Fe_{ox}$ was excluded. Although $Fe_{ox}$ was the single best predictor of the $K_d$ of glyphosate, we obtained a slightly higher accuracy for the $K_d$ of glyphosate in the MLR expression when including $Al_{ox}$ ($R^2 = 0.89$, RMSE = 259.59 mmol kg$^{-1}$) compared to including $Fe_{ox}$ ($R^2 = 0.88$, RMSE = 267.77 mmol kg$^{-1}$). The final MLR expression including Al_ox, $P_{ox}$, and pH is presented in Fig. 4.

Dollinger et al. (2015) suggested that cation exchange capacity and clay content could be applied to determine the $K_d$ across soil samples from Europe, Asia, and North and South America ($K_d$ from 0.83 to 318.82 L kg$^{-1}$). It was also suggested to estimate the amount of sorbed glyphosate from Fe and pH for a set of Danish soil samples (Gimsing et al., 2004). Further, clay, pH, P, and Al were found to be controlling the Freundlich sorption coefficients of soil samples from Argentina (De Gerónimo et al., 2018). Paradelo et al. (2015) found EC, clay and sand contents to be the best predictors of $K_d$ across two Danish agricultural fields ($K_d$ from 161 to 667 L kg$^{-1}$). However, the best subset of soil properties controlling $K_d$ differed when the analysis was performed on each separate field. The best subset of soil properties controlling $K_d$ included pH, clay, Fe, and Olsen P ($K_d$ from 161 to 536 L kg$^{-1}$, clay: 0.06–0.14 kg kg$^{-1}$, OC: 0.02–0.08 kg kg$^{-1}$) for one field, and pH, clay, OC and Olsen P for the other field ($K_d$ from 344 to 667 L kg$^{-1}$, clay: 0.14–0.19 kg kg$^{-1}$, OC: 0.02–0.02 kg kg$^{-1}$).

### 3.3. Qualitative analysis of vis–NIR spectra

It is possible to give a qualified suggestion for which soil properties are affecting the vis–NIR spectra, since several studies have reported which spectral bands are associated with absorption from different chemical bonds and electronic transitions of iron oxides (Clark et al., 1990; Post and Noble, 1993; Stenberg et al., 2010). However, it should be kept in mind that absorption from different organic and inorganic soil constituents is overlapping throughout the spectrum.

The vis–NIR spectra of the two samples exhibiting the highest (3810.35 L kg$^{-1}$; a Brown soil sample) and lowest $K_d$ of glyphosate (13.44 L kg$^{-1}$; a Podzol soil sample) are depicted in Fig. 5. The sample with the highest $K_d$ of glyphosate is also the sample with the highest content of $Fe_{ox}$ (260 mmol kg$^{-1}$) and $Al_{ox}$ (340 mmol kg$^{-1}$) in this dataset and it has a clay content of 0.016 kg kg$^{-1}$ and an OC content of 0.086 kg kg$^{-1}$. The sample with the lowest $K_d$ of glyphosate has one of the lowest $Fe_{ox}$ (12 mmol kg$^{-1}$) and $Al_{ox}$ (14 mmol kg$^{-1}$) contents, a

**Table 2**
Pearson correlation matrix of selected soil properties for 68 soil samples collected across the South Island of New Zealand under pasture.

| | Clay | Silt | Sand | OC[a] | pH | EC[b] | $Al_{ox}$[c] | $Fe_{ox}$[c] | $P_{ox}$[c] | Olsen P[d] | $K_d$[e] |
|---|---|---|---|---|---|---|---|---|---|---|---|
| Clay | 1 | −0.08 | −0.44***[f] | −0.04 | −0.19 | −0.18 | −0.03 | −0.02 | −0.17 | −0.17 | 0.05 |
| Silt | | 1 | −0.86*** | −0.26* | −0.16 | −0.36** | −0.24* | −0.09 | −0.27* | −0.22 | −0.09 |
| Sand | | | 1 | 0.26* | 0.24 | 0.41*** | 0.23 | 0.1 | 0.33** | 0.28* | 0.06 |
| OC | | | | 1 | 0.14 | 0.48*** | 0.3* | 0.26* | 0.27* | 0.76*** | 0.18 |
| pH | | | | | 1 | 0.23 | −0.02 | −0.13 | 0.14 | 0.09 | −0.26* |
| EC | | | | | | 1 | 0.41*** | 0.27* | 0.49*** | 0.51*** | 0.21 |
| $Al_{ox}$ | | | | | | | 1 | 0.91*** | 0.64*** | −0.03 | 0.89*** |
| $Fe_{ox}$ | | | | | | | | 1 | 0.59*** | −0.12 | 0.91*** |
| $P_{ox}$ | | | | | | | | | 1 | 0.31** | 0.37** |
| Olsen P | | | | | | | | | | 1 | −0.19 |
| $K_d$ | | | | | | | | | | | 1 |

[a] OC; Organic carbon.
[b] EC; Electrical conductivity.
[c] $Al_{ox}$, $Fe_{ox}$ and $P_{ox}$; oxalate-extractable fractions of aluminum, iron and phosphorous.
[d] Olsen P: Fraction of available phosphorous.
[e] $K_d$; glyphosate sorption coefficient.
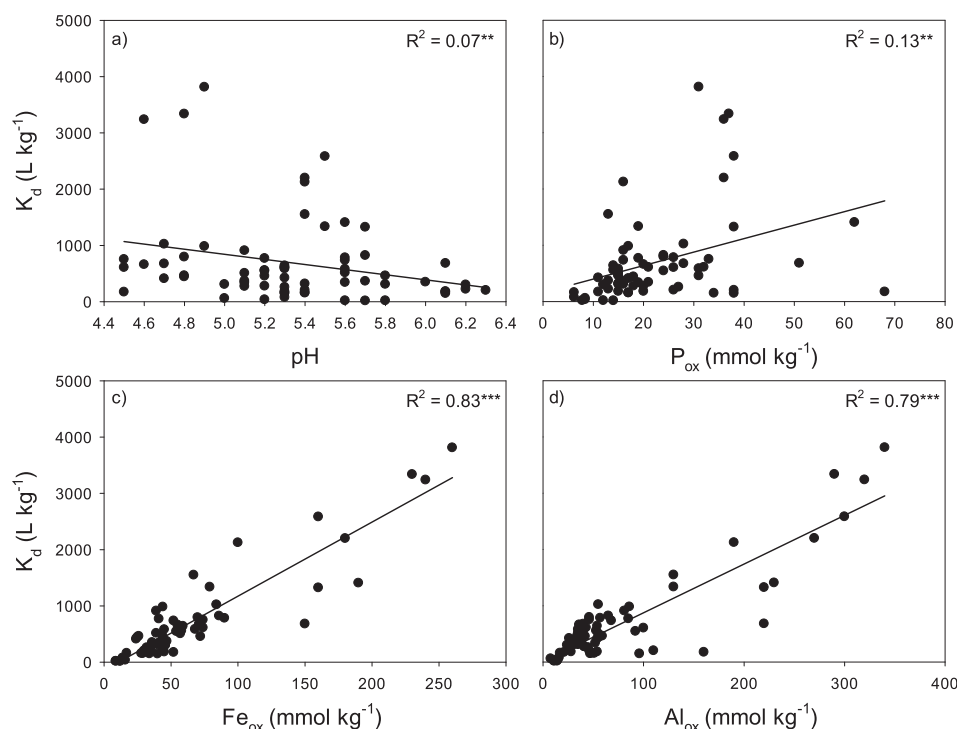[f] Significance levels of *0.05, **0.01, and ***0.001.

**Fig. 3.** The sorption coefficient of glyphosate ($K_d$) as a function of a) pH and oxalate-extractable b) phosphorous ($P_{ox}$), c) iron ($Fe_{ox}$) and d) aluminum ($Al_{ox}$). $R^2$, coefficient of determination.
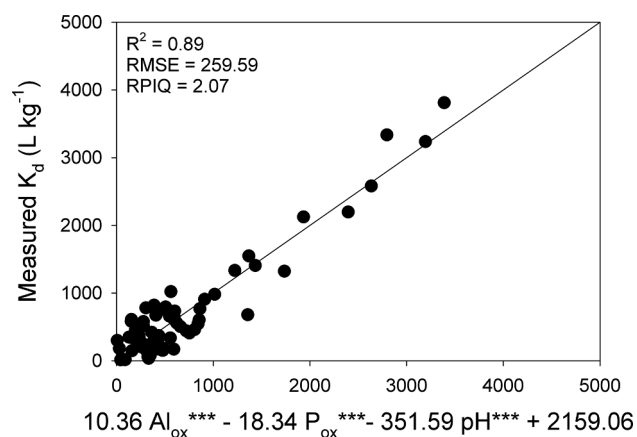


**Fig. 4.** Multiple linear regression analysis for the glyphosate sorption coefficient ($K_d$) including pH and oxalate-extractable aluminum and phosphorous. $R^2$, coefficient of determination; RMSE, root mean square error; RPIQ, ratio of performance to interquartile range.



**Fig. 5.** Visible near-infrared absorbance spectra of the two samples in the dataset with the highest and lowest sorption coefficient of glyphosate ($K_d$). The highlighted region indicates a spectral region affected by overlapping signatures from iron oxides ($Fe_{ox}$) and organic matter (OM).

clay content of $0.075 \, kg \, kg^{-1}$ and the highest OC content of $0.217 \, kg \, kg^{-1}$. The difference in soil composition between these two samples is clear when comparing the spectra. The shape of the spectrum in the visible range was more concave for the soil with the highest $K_d$ due to the high $Fe_{ox}$ content, whereas the spectrum of the soil with lowest $K_d$ was more convex due to the high OC content. A peak which could be caused by the presence of adsorbed and/or lattice OH around 1420 nm (Ben-Dor, 2002) and a peak which could be caused by ad-sorbed water around 1927 nm (Ben-Dor, 2002) were visible for both samples. The sample with the lowest $K_d$ of glyphosate exhibited a local minimum in absorbance around 2222 nm. This absorption band is usually affected by the Al-OH bond (Knadel et al., 2013; Viscarra Rossel and Behrens, 2010).
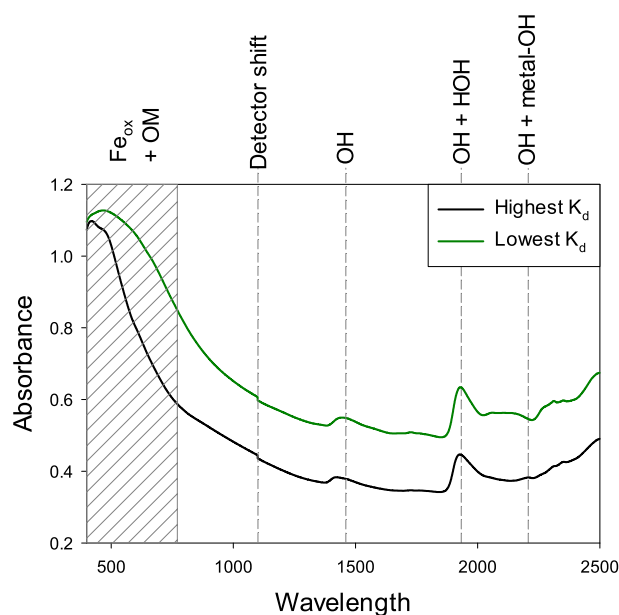
## 3.4. Interval partial least squares regression spectral intervals

With iPLSR, the optimal spectral pretreatment technique for pH prediction was 3rd order detrending followed by SNV, thereby reducing nonlinear trends and scattering effects from the spectrum. For $P_{ox}$, $Fe_{ox}$, $Al_{ox}$, and the $K_d$ of glyphosate, the best results with iPLSR were obtained on spectra with no pretreatments applied (Tables 3 and 4 and Supplementary material, Table 1). A spectral subset including six intervals of adjacent wavelengths for the $K_d$ of glyphosate vis–NIRS

**Table 3**

Spectral intervals from interval partial least squares regression (iPLSR) for pH, oxalate-extractable phosphorous ($P_{ox}$), iron ($Fe_{ox}$), and aluminium ($Al_{ox}$), and the sorption coefficient of glyphosate ($K_d$). For pH, spectral pretreatments included detrending (3rd order) followed by standard normal variate, whereas no pretreatment was applied for the remaining models.

| Parameter | iPLSR intervals (nm) |
| --- | --- |
| pH | 1000–1050 and 1900–2000 |
| $P_{ox}$ | 580–700, 1000–1060, 1120–1180, 1420–1480, 1720–1780, 1900–1960, 2260–2320, and 2380–2440 |
| $Fe_{ox}$ | 400–440, 480–520, 840–880, 1360–1400, 1680–1720, 1760–1800, 1880–1920, 2280–2320, and 2400–2480 |
| $Al_{ox}$ | 550–600, 1000–1100, and 2100–2200 |
| $K_d$ | 400–440, 560–600, 640–680, 1280–1320, 2160–2240, and 2280–2360 |

**Table 4**

Best performing models using interval partial least squares regression (iPLSR) for pH, oxalate extractable fractions of phosphorous ($P_{ox}$), iron ($Fe_{ox}$), and aluminum ($Al_{ox}$), and glyphosate sorption coefficients ($K_d$).

| Parameter | Spectral pretreatment | Factors | RMSEC[a] | R[2] (C)[b] | RMSECV[c] | R[2] (CV)[d] | RPIQ[e] |
| --- | --- | --- | --- | --- | --- | --- | --- |
| pH | Detrending + SNV[f] | 7 | 0.62 | 0.28 | 0.32 | 0.50 | 1.58 |
| $P_{ox}$ | None | 15 | 3.58 | 0.91 | 4.86 | 0.84 | 2.67 |
| $Fe_{ox}$ | None | 14 | 9.83 | 0.97 | 14.31 | 0.93 | 2.48 |
| $Al_{ox}$ | None | 13 | 15.22 | 0.96 | 20.70 | 0.94 | 2.43 |
| $K_d$ | None | 14 | 139.78 | 0.97 | 207.58 | 0.93 | 2.59 |

[a] Root mean square error of calibration.
[b] Regression coefficient from calibration.
[c] Root mean square error of cross-validation.
[d] Regression coefficient from cross-validation.
[e] Ratio of performance to interquartile range.
[f] Standard normal variate.

prediction was selected and included intervals from 400 to 440 nm, 560 to 600 nm, 640 to 680 nm, 1280 to 1320 nm, 2160 to 2240 nm, and 2280 to 2360 nm (Table 3).

The first three iPLSR intervals from 400 to 440 nm, 560 to 600 nm, and 640 to 680 nm are located in spectral regions that are affected by iron oxides, such as goethite (e.g., around 420, 434, and 650 nm) and hematite (e.g., at 404, 529 and 650 nm) (Knadel et al., 2013; Stenberg et al., 2010; Viscarra Rossel and Behrens, 2010; Viscarra Rossel et al., 2006). Further, the iPLSR model for $Fe_{ox}$ is utilizing a similar spectral interval from 400 to 440 nm, which emphasizes that this spectral interval contains useful information about iron oxides. The iPLSR interval from 640 to 680 nm used for predicting the $K_d$ is overlapping spectral intervals used for predicting $P_{ox}$ (580–700 nm) and $Al_{ox}$ (550–600 nm), which might reflect the intercorrelation to iron oxides for these soil parameters (Table 2). The iPLSR interval from 1280 to 1320 nm is overlapping a spectral range affected by OH bonds associated with minerals (Hunt, 1977) and some species of OM. It seems more probable that the model is utilizing information from soil moisture than OM due to the low correlation between the $K_d$ of glyphosate and OC (Table 2). However, some literature states that OM is affecting the $K_d$ of glyphosate (Borggaard and Gimsing, 2008; Dollinger et al., 2015; Gerritse et al., 1996; Paradelo et al., 2015; Piccolo et al., 1996; Vereecken, 2005), and therefore the quality and quantity of OM might also be affecting this vis–NIRS model. The iPLSR interval from 2160 to 2240 nm is located in a spectral region with signatures from the OH stretch and metal-OH bend (Viscarra Rossel and Behrens, 2010), which corroborates with the fact that the iPLSR model for $Al_{ox}$ utilizes an overlapping spectral interval from 2100 to 2200 nm. The last spectral interval from 2280 to 2360 nm is located in a spectral region affected by different clay minerals and species of organic matter (Viscarra Rossel and Behrens, 2010), and this region was also important for the $Fe_{ox}$ prediction (iPLSR interval from 2280 to 2320 nm).

### 3.5. Vis–NIRS models

The pH, $P_{ox}$, $Fe_{ox}$, and $Al_{ox}$ were vis–NIRS-predicted to test whether vis–NIRS could predict basic soil properties controlling the $K_d$ of

glyphosate (Table 4; Fig. 6). Using spectral intervals selected with iPLSR improved all four models as compared to using the entire spectrum (Supplementary material, Table 1).

The pH was estimated with moderate accuracy in cross-validation ($R^2$ of 0.50, RMSECV of 0.32, RPIQ = 1.58; Fig. 6a). Since pH is not spectrally active the ability of vis–NIRS to estimate pH might be caused by intercorrelations of pH with OC and clay contents (Wetterlind and Stenberg, 2010). Thus, the low accuracy for pH determination might be caused by the fact that pH possess a very low correlation to OC and clay contents (Table 2). The $P_{ox}$ content was predicted with an $R^2$ of 0.84, an RMSECV of 4.86 mmol kg$^{-1}$, and an RPIQ value of 2.67 (Fig. 6b). Another study predicted $P_{ox}$ with a $R^2$ of 0.79 and an RMSEP of 4.81 mmol L$^{-1}$ ($P_{ox}$ range from 0.99 to 39.55 mmol L$^{-1}$) (Kawamura et al., 2019). Since phosphorous does not carry any direct spectral signatures, the vis–NIRS-prediction of $P_{ox}$ is possible because it correlates to soil components that are spectrally active (Stenberg et al., 2010), as for example $Fe_{ox}$ and $Al_{ox}$ for this dataset (Table 2). The $Fe_{ox}$ content was predicted well ($R^2$ of 0.93, RMSECV of 14.31 mmol kg$^{-1}$, RPIQ of 2.48; Fig. 6c). This accuracy is higher as compared with the study of Xu et al. (2018), in which $Fe_{ox}$ was predicted with an $R^2$ of 0.85 and an RMSEP of 17.27 mmol kg$^{-1}$ ($Fe_{ox}$ range from 1.61 to 222.58 mmol L$^{-1}$). The $Al_{ox}$ prediction was also successful ($R^2$ of 0.94, RMSECV of 20.70 mmol kg$^{-1}$, RPIQ of 2.43; Fig. 6d), with a similar RPIQ as was obtained for the $Fe_{ox}$ prediction. Compared to Paradelo et al. (2016) where $Al_{ox}$ was predicted with an $R^2$ of 0.88 and an RMSECV of 4.85 mmol kg$^{-1}$ the $R^2$ was higher in this study, but the RMSECV was much lower in Paradelo et al. (2016), possibly due to a higher variability in our samples.

As Supplementary information, we successfully predicted OC content ($R^2$ of 0.64, RMSECV of 0.018 kg kg$^{-1}$), EC ($R^2$ of 0.74, RMSECV of 1.15 mS cm$^{-1}$), and Olsen P ($R^2$ of 0.64, RMSECV of 21.34 mmol kg$^{-1}$) using the entire spectrum. However, the soil texture could not be predicted, possibly due to the high variability in mineralogy of this dataset.

The $K_d$ of glyphosate was successfully predicted, resulting in an $R^2$ of 0.93, an RMSECV of 207.58, and an RPIQ of 2.59 (Fig. 7; Table 4). Using iPLSR improved the model accuracy for both pH, $P_{ox}$, $Fe_{ox}$, $Al_{ox}$ and the $K_d$ of glyphosate as compared to using the entire spectrum.
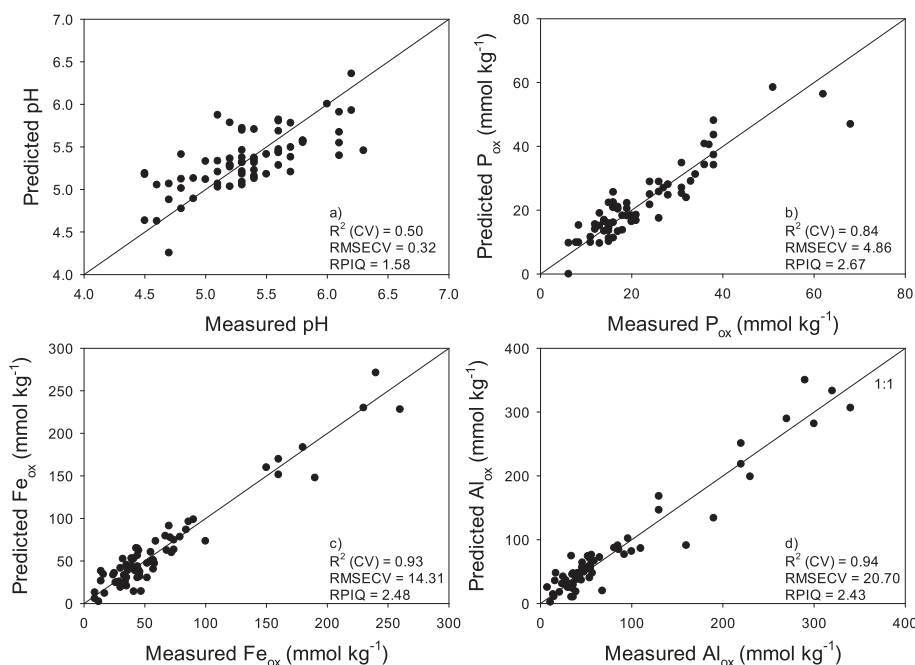
**Fig. 6.** Visible near-infrared spectroscopy predictions of a) pH and oxalate-extractable fractions of b) phosphorous ($P_{ox}$), c) iron ($Fe_{ox}$), and d) aluminum ($Al_{ox}$) using interval partial least squares regression. $R^2$, coefficient of determination; RMSECV, root mean square error of cross-validation; RPIQ, ratio of performance to interquartile range.

Compared to Paradelo et al. (2016) who obtained an $R^2$ of 0.79 and an RMSECV of 45.54 L kg$^{-1}$ using the full spectrum, we generated a higher $R^2$ and a higher error due to the large range in $K_d$ of glyphosate present in our dataset.

## 4. Conclusion

This study included soil samples from New Zealand, covering a wide range of several soil properties. The key drivers for the variation in glyphosate sorption coefficient ($K_d$) included pH, and oxalate-extractable fractions of phosphorous ($P_{ox}$), iron ($Fe_{ox}$) and aluminum ($Al_{ox}$). Further, the best subset for a multiple linear regression for the $K_d$ of glyphosate consisted of $Al_{ox}$, $P_{ox}$ and pH.

We successfully established vis–NIRS prediction models for the soil properties controlling $K_d$ of glyphosate. Based on RPIQ values, the $P_{ox}$ vis–NIRS-model obtained the highest accuracy (RPIQ of 2.67) followed by the models for $Fe_{ox}$ (RPIQ of 2.48), $Al_{ox}$ (RPIQ of 2.43) and pH (RPIQ of 1.58).

The $K_d$ of glyphosate was best and successfully predicted with a

subset of the spectrum, found by interval partial least squares regression (iPLSR) including information from iron oxides, organic matter species, soil moisture, and aluminum oxides.

Based on the findings of this study and considering our dataset, it was more accurate to apply vis–NIRS to predict $K_d$ of glyphosate than MLR analysis utilizing basic soil properties. Our study documents that the $K_d$ of glyphosate can be vis–NIRS-predicted at large scale and not only at field-scale. The applicability of vis–NIRS for the prediction of $K_d$ of glyphosate adds a functional soil property to the list of numerous basic and functional soil properties that can be obtained from a single vis–NIR spectrum.

### Declaration of Competing Interest

The authors declare that they have no known competing financial interests or personal relationships that could have appeared to influence the work reported in this paper.

### Acknowledgements

### Appendix A. Supplementary data

Supplementary data to this article can be found online at https://doi.org/10.1016/j.geoderma.2019.114009.

### References

Al-Rajab, A.J., Amellal, S., Schlavon, M., 2008. Sorption and leaching of $^{14}$C-glyphosate in agricltural soils. Agron. Sustainable Dev. 28, 419–428. https://doi.org/10.1051/agro:2008014.

Arias-Estévez, M., López-Periago, E., Martínez-Carballo, E., Simal-Gándara, J., Mejuto, J.C., García-Río, L., 2008. The mobility and degradation of pesticides in soils and the pollution of groundwater resources. Agric. Ecosyst. Environ. 123 (4), 247–260. https://doi.org/10.1016/j.agee.2007.07.011.

Barnes, R.J., Dhanoa, M.S., Lister, S.J., 1989. Standard normal variate transformation and de-trending of near-infrared diffuse reflectance spectra. J. Appl. Spectrosc. 43 (5),
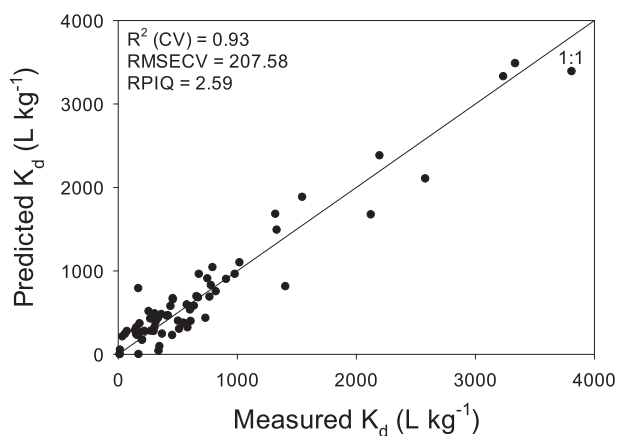


**Fig. 7.** Visible near-infrared spectroscopy predictions of the glyphosate sorption coefficient ($K_d$) using spectral intervals determined using interval partial least squares regression (iPLSR). $R^2$, coefficient of determination; RMSECV, root mean square error of cross-validation; RPIQ, ratio of performance to interquartile range.

772–777. https://doi.org/10.1366/0003702894202201.

Bellon-Maurel, V., Fernandez-Ahumada, E., Palagos, B., Roger, J.M., McBratney, A., 2010. Critical review of chemometric indicators commonly used for assessing the quality of the prediction of soil attributes by NIR spectroscopy. TrAC, Trends Anal. Chem. 29 (9), 1073–1081. https://doi.org/10.1016/j.trac.2010.05.006.

Ben-Dor, E., 2002. Quantitative remote sensing of soil properties. Adv. Agron. 75, 173–243. https://doi.org/10.1016/S0065-2113(02)75005-0.

Ben-Dor, E., Banin, A., 1995. Near-infrared analysis as a rapid method to simultaneously evaluate several soil properties. Soil Sci. Soc. Am. J. 59 (2), 364–372. https://doi.org/10.2136/sssaj1995.03615995005900020014x.

Bengtsson, S., Berglöf, T., Kylin, H., 2007. Near infrared reflectance spectroscopy as a tool to predict pesticide sorption in soil. Bull. Environ. Contamin. Toxicol. 78 (5), 295–298. https://doi.org/10.1007/s00128-007-9167-x.

Blakemore, L., Searle, P.L., Dalby, B.K., 1987. Methods for chemical analysis of soils. New Zealand Soil Bureau Scientific Report No. 80, New Zealand Soil Bureau, Wellington.

Borggaard, O.K., 2011. Does phosphate affect soil sorption and degradation? – a review. Trends Soil Sci. Plant Nutr. J. 2 (1), 16–27.

Borggaard, O.K., Gimsing, A.L., 2008. Fate of glyphosate in soil and the possibility of leaching to ground and surface waters: a review. Pest Manage. Sci. 64, 441–456. https://doi.org/10.1002/ps.1512.

Chang, C.W., Laird, D.A., Mausbach, M.J., Hurburgh, C.R., 2001. Near-infrared reflectance spectroscopy-principal components regression analyses of soil properties. Soil Sci. Soc. Am. J. 65 (2), 480–490. https://doi.org/10.2136/sssaj2001.652480x.

Clark, R.N., 1999. Spectroscopy of rocks and minerals and principles of spectroscopy. In: Rencz, A.N. (Ed.), Remote Sensing for the Earth Sciences: Manual of Remote Sensing. John Wiley & Sons, Chichester, UK, pp. 3–58.

Clark, R.N., King, T.V.V., Klejwa, M., Swayze, G.A., Vergo, N., 1990. High spectral resolution reflectance spectroscopy of minerals. J. Geophys. Res. 95 (B8), 12653–12680. https://doi.org/10.1029/JB095iB08p12653.

Close, M.E., Skinner, A., 2012. Sixth national survey of pesticides in groundwater in New Zealand. N. Z. J. Mar. Freshwater Res. 46 (4), 443–457. https://doi.org/10.1080/00288330.2012.707131.

De Gerónimo, E., Aparicio, V.C., Costa, J.L., 2018. Glyphosate sorption to soils of Argentina. Estimation of affinity coefficient by pedotransfer function. Geoderma 322, 140–148. https://doi.org/10.1016/j.geoderma.2018.02.037.

de Jong, S., 1993. SIMPLS: an alternative approach to partial least squares regression. Chemom. Intell. Lab. Syst. 18 (3), 251–263. https://doi.org/10.1016/0169-7439(93)85002-X.

de Jonge, H., de Jonge, L.W., 1999. Influence of pH and solution composition on the sorption of glyphosate and prochloraz to a sandy loamy soil. Chemosphere 39, 753–763. https://doi.org/10.1016/S0045-6535(99)00011-9.

de Jonge, H., de Jonge, L.W., Jacobsen, O.H., 2000. [$^{14}$C]Glyphosate transport in undistrubed topsoil columns. Pest Manage. Sci. 56, 909–915. https://doi.org/10.1002/1526-4998(200010)56:10<909::AID-PS227>3.0.CO;2-5.

de Jonge, H., de Jonge, L.W., Jacobsen, O.H., Yamaguchi, T., Moldrup, P., 2001. Glyphosate sorption in soils of different pH and phosphorous content. Soil Sci. 166, 230–238. https://doi.org/10.1097/00010694-200104000-00002.

de Jonge, L.W., Kjaergaard, C., Moldrup, P., 2004a. Colloids and colloid-facilitated transport of contaminants in soils: an introduction. Vadose Zone J. 3 (2), 321–325. https://doi.org/10.2136/vzj2004.0321.

de Jonge, L.W., Moldrup, P., Rubaek, G.H., Schelde, K., Djurhuus, J., 2004b. Particle leaching and particle-facilitated transport of phosphorus at field scale. Vadose Zone J. 3 (2), 462–470. https://doi.org/10.2113/3.2.462.

Dollinger, J., Dagés, C., Voltz, M., 2015. Glyphosate sorption to soils and sediments predicted by pedotransfer functions. Environ. Chem. Lett. 13 (3), 293–307. https://doi.org/10.1007/s10311-015-0515-5.

Farenhorst, A., Papiernik, S.K., Saiyed, I., Messing, P., Stephens, K.D., Schumacher, J.A., Lobb, D.A., Li, S., Lindstrom, M.J., Schumacher, T.E., 2008. Herbicide sorption coefficients in relation to soil properties and terrain attributes on a cultivated prairie. J. Environ. Qual. 37 (3), 1201–1208. https://doi.org/10.2134/jeq2007.0109.

Forouzangohar, M., Cozzolino, D., Kookana, R.S., Smernik, R.J., Forrester, S.T., Chittleborough, D.J., 2009. Direct comparison between visible near- and mid-infrared spectroscopy for describing diuron sorption in soils. Environ. Sci. Technol. 43 (11), 4049–4055. https://doi.org/10.1021/es8029945.

Gerritse, R.G., Beltran, J., Hernandez, F., 1996. Adsorption of atrazine, simazine, and glyphosate in soils of the Gnangara Mound, Western Australia. Aust. J. Soil Res. 34 (4), 599–607. https://doi.org/10.1071/Sr9960599.

Gimsing, A.L., Borggaard, O.K., 2010. Effect of phosphate on the adsorption of glyphosate in soils, clay minerals and oxides. Int. J. Environ. Anal. Chem. 82, 545–552. https://doi.org/10.1080/0306731021000062964.

Gimsing, A.L., Borggaard, O.K., Bang, M., 2004. Influence of soil composition on adsorption of glyphosate and phosphate by contrasting Danish surface soils. Eur. J. Soil Sci. 55 (1), 183–191. https://doi.org/10.1046/j.1365-2389.2003.00585.x.

Glass, R.L., 1987. Adsorption of glyphosate by soils and clay minerals. J. Agric. Foood. Chem. 35, 497–500. https://doi.org/10.1021/jf00076a013.

Hermansen, C., Knadel, M., Moldrup, P., Greve, M.H., Gislum, R., de Jonge, L.W., 2016. Visible–near-infrared spectroscopy can predict the clay/organic carbon and mineral fines/organic carbon ratios. Soil Sci. Soc. Am. J. 80, 1486–1495. https://doi.org/10.2136/sssaj2016.05.0159.

Hermansen, C., Knadel, M., Moldrup, P., Greve, M.H., Karup, D., de Jonge, L.W., 2017. Complete soil texture is accurately predicted by visible near-infrared spectroscopy. Soil Sci. Soc. Am. J. 81 (4), 758–769. https://doi.org/10.2136/sssaj2017.02.0066.

Hermansen, C., Moldrup, P., Müller, K., Jensen, P.W., Van den Dijssel, C., Jeyakumar, P., de Jonge, L.W., 2019. Organic carbon content controls the severity of water repellency and the critical moisture level across New Zealand pasture soils. Geoderma 338, 281–290. https://doi.org/10.1016/j.geoderma.2018.12.007.

Hewitt, A.E., 2010. New Zealand Soil Classification. Landcare Research Science Series No. 1. Lincoln, third ed. Manaaki Whenua Press.

Hunt, G.R., 1977. Spectral signatures of particulate minerals in the visible and near infrared. Geophysics 42 (3), 501–513. https://doi.org/10.1190/1.1440721.

IUSS Working Group WRB, 2006. World Reference Base for Soil Resources 2006. A Framework for International Classification, Correlation and Communication, second ed. FAO, Rome.

Katuwal, S., Hermansen, C., Knadel, M., Moldrup, P., Greve, M.H., de Jonge, L.W., 2018a. Combining X-ray computed tomography and visible near-infrared spectroscopy for prediction of soil structural properties. Vadose Zone J. 17 (1). https://doi.org/10.2136/vzj2016.06.0054.

Katuwal, S., Knadel, M., Moldrup, P., Norgaard, T., Greve, M.H., de Jonge, L.W., 2018b. Visible-near-infrared spectroscopy can predict mass transport of dissolved chemicals through intact soil. Sci. Rep. 8. https://doi.org/10.1038/s41598-018-29306-9.

Kawamura, K., Tsujimoto, Y., Nishigaki, T., Andriamananjara, A., Rabenarivo, M., Asai, H., Rakotoson, T., Razafimbelo, T., 2019. Laboratory visible and near-infrared spectroscopy with genetic algorithm-based partial least squares regression for assessing the soil phosphorus content of upland and lowland rice fields in Madagascar. Remote Sens. 11 (5), 506. https://doi.org/10.3390/rs11050506.

Kjær, J., Olsen, P., Ullum, M., Grant, R., 2005. Leaching of glyphosate and amino-methylphosphonic acid from Danish agricultural field sites. J. Environ. Qual. 34 (2), 608–620. https://doi.org/10.2134/jeq2005.0608.

Knadel, M., Arthur, E., Weber, P., Moldrup, P., Greve, M.H., Chrysodonta, Z.P., de Jonge, L.W., 2018. Soil specific surface area determination by visible near-infrared spectroscopy. Soil Sci. Soc. Am. J. 82 (5), 1046–1056. https://doi.org/10.2136/sssaj2018.03.0093.

Knadel, M., Masis-Meléndez, F., de Jonge, L.W., Moldrup, P., Arthur, E., Greve, M.H., 2016. Assessing soil water repellency of a sandy field with visible near infrared spectroscopy. J. Near Infrared Spectrosc. 24 (3), 215–224. https://doi.org/10.1255/jnirs.1188.

Knadel, M., Rossel, R.A.V., Deng, F., Thomsen, A., Greve, M.H., 2013. Visible-near infrared spectra as a proxy for topsoil texture and glacial boundaries. Soil Sci. Soc. Am. J. 77 (2), 568–579. https://doi.org/10.2136/sssaj2012.0093.

Manktelow, D., Stevens, P., Walker, J., Gurnsey, S., Park, N., Zabkiewicz, J., Teulon, D., Rahman, A., 2004. Trends in pesticide use in New Zealand: 2004. Client Report HortResearch, Wellington, pp. 78.

Ministry for Primary Industries, 2015. Glyphosate – Overview of use and monitoring in New Zealand.

Norgaard, T., Moldrup, P., Ferré, T.P.A., Olsen, P., Rosenbom, A.E., de Jonge, L.W., 2014. Leaching of glyphosate and aminomethylphosphonic acid from an agricultural field over a twelve-year period. Vadose Zone J. 13 (10). https://doi.org/10.2136/vzj2014.05.0054.

Norgaard, T., Moldrup, P., Olsen, P., Vendelboe, A.L., Iversen, B.V., Greve, M.H., Kjaer, J., de Jonge, L.W., 2013. Comparative mapping of soil physical-chemical and structural parameters at field scale to identify zones of enhanced leaching risk. J. Environ. Qual. 42 (1), 271–283. https://doi.org/10.2134/jeq2012.0105.

Nørgaard, L., Saudland, A., Wagner, J., Nielsen, J.P., Munck, L., Engelsen, S.B., 2000. Interval partial least-squares regression (iPLS): a comparative chemometric study with an example from near-infrared spectroscopy. Appl. Spectrosc. 54 (3), 413–419. https://doi.org/10.1366/0003702001949500.

Olsen, S.R., 1954. Estimation of Available Phosphorous in Soils by Extraction with Sodium Bicarbonate. U. S. Govt. Orint. Off., Washington.

Paradelo, M., Hermansen, C., Knadel, M., Moldrup, P., Greve, M.H., de Jonge, L.W., 2016. Field-scale predictions of soil contaminant sorption using visible-near infrared spectroscopy. J. Near Infrared Spectrosc. 24, 281–291. https://doi.org/10.1255/jnirs.1228.

Paradelo, M., Norgaard, T., Moldrup, P., Ferré, T.P.A., Kumari, K.G.I.D., Arthur, E., de Jonge, L.W., 2015. Prediction of the glyphosate sorption coefficient across two loamy agricultural fields. Geoderma 259–260, 224–232. https://doi.org/10.1016/j.geoderma.2015.06.011.

Piccolo, A., Celano, G., Conte, P., 1996. Adsorption of glyphosate by humic substances. J. Agric. Food Chem. 44 (8), 2442–2446. https://doi.org/10.1021/jf950620x.

Post, J.L., Noble, P.N., 1993. The near-infrared combination band frequencies of dioctahedral smectites, micas and illites. Clays Clay Miner. 6, 639–644.

Savitzky, A., Golay, M.J.E., 1964. Smoothing and differentiation of data by simplified least squares procedures. Anal. Chem. 36 (8), 1627–1639. https://doi.org/10.1021/ac60214a047.

Schoumans, O.F., 2000. Determination of the degree of phosphate saturation in noncalcareous soils. In: Pierzynski, G.M. (Ed.), Methods of Phosphorus Analysis for Soils, Sediments, Residuals, and Waters. Raleigh NC, USA, pp. 31–34.

Sheals, J., Sjöberg, S., Persson, P., 2002. Adsorption of glyphosate on goethite: molecular characterization of surface complexes. Environ. Sci. Technol. 36 (14), 3090–3095. https://doi.org/10.1021/es010295w.

Soares, A.A., Moldrup, P., Minh, L.N., Vendelboe, A.L., Schjonning, P., de Jonge, L.W., 2013. Sorption of phenanthrene on agricultural soils. Water Air Soil Pollut. 224 (4), 1519. https://doi.org/10.1007/s11270-013-1519-z.

Sprankle, P., Meggitt, W.F., Penner, D., 1975. Adsorption, mobility, and microbial degradation of glyphosate in the soil. Weed Sci. 23 (3), 229–234.

Stenberg, B., Viscarra Rossel, R.A., Mouazen, A.M., Wetterlind, J., 2010. Visible and near infrared spectroscopy in soil science. Adv. Agron. 107, 163–512.

Stewart, M., Olsen, G., Hickey, C.W., Ferreira, B., Jelić, A., Petrović, M., Barcelo, D., 2014. A survey of emerging contaminants in the estuarine receiving environment around Auckland, New Zealand. Sci. Total Environ. 468–469, 202–210. https://doi.org/10.1016/j.scitotenv.2013.08.039.

Vereecken, H., 2005. Mobility and leaching of glyphosate: a review. Pest Manage. Sci. 61 (12), 1139–1151. https://doi.org/10.1002/ps.1122.

Viscarra Rossel, R.A., Behrens, T., 2010. Using data mining to model and interpret soil diffuse reflectance spectra. Geoderma 158 (1–2), 46–54. https://doi.org/10.1016/j.geoderma.2009.12.025.

Viscarra Rossel, R.A., Walvoort, D.J.J., McBratney, A.B., Janik, L.J., Skjemstad, J.O., 2006. Visible, near infrared, mid infrared or combined diffuse reflectance spectroscopy for simultaneous assessment of various soil properties. Geoderma 131 (1–2), 59–75. https://doi.org/10.1016/j.geoderma.2005.03.007.

Wetterlind, J., Stenberg, B., 2010. Near-infrared spectroscopy for within-field soil characterization: small local calibrations compared with national libraries spiked with local samples. Eur. J. Soil Sci. 61 (6), 823–843. https://doi.org/10.1111/j.1365-2389.2010.01283.x.

Xu, S., Zhao, Y., Wang, M., Shi, X., 2018. Quantification of different forms of iron from intact soil cores of paddy fields with vis-NIR spectroscopy. Soil Sci. Soc. Am. J. 82 (6), 1497–1511. https://doi.org/10.2136/sssaj2018.01.0014.

Zou, X., Zhao, J., Povey, M.J.W., Holmes, M., Mao, H., 2010. Variables selection methods in near-infrared spectroscopy. Anal. Chim. Acta 667 (1–2), 14–32. https://doi.org/10.1016/j.aca.2010.03.048.